DSI DATA SCIENCE AND INFORMETRICS

RESEARCH ARTICLE

Manifold sorting feature selection for emotion recognition

Zhaowen Xiao[a], Qingshan She[a, b*], Lei Chen[a], Yuliang Ma[a, b]

a. HDU-ITMO Joint Institute, Hangzhou Dianzi University, Hangzhou, China

b. School of Automation, Hangzhou Dianzi University, Hangzhou, China

ABSTRACT

Feature selection plays a crucial role in electroencephalography (EEG)-based emotion recognition. Currently, there is limited research connecting feature selection with specific brain regions in EEG emotion recognition, and the application of transfer learning in feature selection is also scarce. This paper proposes a novel manifold sorting feature selection (MSFS) method, and its corresponding multi-source classification framework. MSFS selects channel features most similar to the T7 and T8 channels, which are highly related to each emotion category, using effective manifold-based similarity ranking. The selected features are combined and used for prediction and classification. Experimental results demonstrate that the average classification accuracy of the MSFS method combined with SVM on the SEED, and SEED-IV is 77.63%, and 53.65%, which are 1.26%, and 2.90% higher than the SVM without MSFS. Furthermore, MSFS is compared with other feature selection methods, and the results show that MSFS achieves the best performance when used in conjunction with transfer learning for classification.

KEYWORDS

Brain-computer interfaces; Feature selection; Cross-subject; Emotion recognition

1 Introduction

Emotion recognition technology based on electroencephalography (EEG) signal analysis has become crucial in artificial intelligence. It exhibits significant potential in emotional health care, human-computer interaction, and multimedia content recommendation (X Li et al., 2022). Research has shown that patients' emotions have a significant impact on rehabilitation. Positive emotions are beneficial for physical and mental health, enhance happiness, and promote the recovery of bodily functions; while negative emotions can easily lead to problems such as depression, anxiety, and insomnia, and long-term maintenance of this state may hinder recovery (Huang et al., 2019). Interactivity is an important feature of virtual reality, where emotions influence human interaction behavior and can reflect several emotional states (Dalgarno & Lee,

*Corresponding author: qsshe@hdu.edu.cn

2010). Therefore, emotion recognition can enable interaction systems to analyze the deep meaning of behavior further, and the system can provide feedback control based on the recognized human emotional state, targeted to meet user needs, and promote the intelligent development of human-computer interaction (Makantasis et al.,2023). Derdiyok & Akbulut (2023) proposed a novel video abstract based on physiological signals provided by emotional stimuli in social media. Reading such abstracts can help you understand the importance of quickly judging likes, ratings, comments, and more.

Human physiological signals often change with changes in emotions. Physiological signals can reflect more authentic emotional states than other emotion recognition modes. Other emotion recognition modes, such as facial expressions, often have inaccurate representations and are easily disguised, so physiological signals are important input signals for emotion recognition (Lin & Li, 2023). Moontaha et al. (2023) developed a real-time emotion classification pipeline using non-invasive portable EEG sensors based on directly measuring electrical correlation from the brain, achieving real-time prediction in real-time scenes with delayed labels while constantly updating. Tao et al. (2023) proposed an attention-based convolutional recurrent neural network (ACRNN) by obtaining useful information on EEG channels and time, which extracts more discriminative features from EEG signals and improves emotion recognition accuracy. Cheng et al. (2022) proposed a hybrid EEG modeling method to simulate human dynamic emotional behavior by considering brain electrodes' positional connectivity and contextual dependence. The method introduced an attention mechanism to combine the multi-domain spatial transformer module and the dynamic temporal transformer module, improving the classification performance of emotion recognition. Although EEG-based emotion recognition has the above advantages, some things could still be improved. Ahmed et al. (2023) proposed the InvBase algorithm in EEG signal preprocessing, which improves recognition performance by removing baseline power before extracting features that remain unchanged regardless of the topic. Zhong et al. (2023) proposed a new emotion recognition framework based on EEG to address the problem of non-linear and non-stationary EEG signals making it difficult to analyze and extract effective emotional information from these signals. This framework achieved excellent performance using the tunable Q-factor wavelet transform feature extraction method, a new spatiotemporal representation of multi-channel EEG signals, and a hybrid convolutional recurrent neural network. EEG-based emotion recognition needs to be fixed. The volume conduction effect of the human head introduces inter-channel dependence and leads to a high correlation of information between most EEG features. These highly correlated EEG features cannot provide additional useful information, and they reduce emotion recognition performance. Xu et al. (2023) proposed the global redundancy minimization in orthogonal regression method in orthogonal regression to effectively evaluate the correlation between all EEG features. The work of this article also provides a method to solve this problem.

Emotion recognition based on EEG includes several modules, such as obtaining EEG data, data preprocessing, feature extraction and selection, and classification (Shu et al., 2018). Feature extraction and selection have always been important research directions in emotion recognition. Existing methods can be divided into two categories: manually designed and deep learning-based. In manually scheduled feature extraction and selection, Chen et al. (2021) considered an EEG to be an unstable and rapidly changing voltage signal. Therefore, they proposed an emotion recognition feature extraction method based on EEG microstates. The method addresses the problem of significant feature variations in the extracted EEG features due to gradual changes in emotional states. By utilizing microstate analysis, the method captures the important spatiotemporal characteristics of EEG signals and extracts microstate features as novel spatiotemporal features, thereby improving the emotion recognition performance of EEG signals. She et al. (2023a) proposed a multi-source transfer learning framework that maintains the domain invariance of EEG features and reduces data drift by embedding all samples into a brand-new feature space. Yin et al. (2020) proposed a novel locally robust feature selection (LRFS) method to identify common EEG features among multiple subjects. In the LRFS framework, the extracted EEG features are first modeled using probability density estimation. The inter-individual consistency of the EEG features is described by evaluating the similarity of all density functions between each pair of subjects. The obtained consistency determines the locally robust EEG features. The LRFS feature selection method performs well on publicly available datasets, but the features identified by LRFS are not adapted to specific domain data.

Feature extraction and selection methods based on deep learning rely on automatic learning using deep neural networks, such as convolutional neural networks, recurrent neural networks, and autoencoders (Zhang et al., 2022; Zhang et al., 2019; Yin et al., 2017). In addition, Lv et al. (2022) combined frequency-domain features, spatial information, and frequency band features of multi-channel EEG signals to generate a novel emotion recognition network with multi-band EEG topography. She et al. (2023b) proposed a new emotion recognition method based on a multisource associate domain adaptation network, considering domain-invariant and domain-specific features. The domain-specific features were extracted using the one-to-one associate domain adaptation. Song et al. (2020) proposed a method of modeling multi-channel EEG features using graphs, considering the inherent relationship between EEG channels in the emotion recognition process, which improved classification accuracy. Şengür & Siuly (2020) proposed an efficient emotion recognition framework based on deep learning. In this framework, signals are preprocessed with low-pass filtering to remove noise, and the Delta frequency is extracted and transformed into EEG rhythm images through continuous wavelet transform. Then, pre-trained convolutional neural network models are used to discover in-depth features, followed by selecting deep features using MobileNetv2. Finally, the selected features are classified using the long short-term memory method, achieving good performance. Deep learning models have strong feature learning capabilities and can extract complex high-level features. However, these methods often require much-labeled data and computational resources to train the model. In summary, the human-designed method relies on domain experts' experience and knowledge, and often requires extensive experimental validation, while the deep learning-based method can adaptively learn the expression in the data without much human intervention but requires a large amount of data to train the model.

This paper proposes the manifold sorting feature selection (MSFS) algorithm to address the problem of selecting emotion features suitable for specific domains. There are two key technologies in MSFS:

1) MSFS selects other channel features that are most correlated with the EEG emotion channels discovered in existing studies through manifold sorting.

2) MSFS processes the labeled target data based on the selected features from each source domain to obtain its classification accuracy on different source domains. Then, it uses accuracy as a criterion to determine the similarity between the target domain and other source domains,

while assigning weights to each source domain, enabling it to adapt to multi-source classification scenarios.

The rest of this paper is organized as follows. Section 2 describes the details of the used datasets and proposed algorithm. In Section 3, the experiments verify the performance of our method compared with several state-of-the-art approaches. The discussions are given in Section 4. Finally, the conclusion is given in Section 5.

2. Material and methods

2.1 Dataset description

To verify the effectiveness of the proposed model, three public datasets are used for experiments, including SEED, SEED-IV and DEAP. The details are given as follows.

(1) SEED (Duan et al., 2013; Zheng & Lu, 2015): Fifteen Chinese film clips, consisting of 5 positive emotions, 5 neutral emotions, and 5 negative emotions, were utilized as stimuli to elicit corresponding emotional responses from the participants. A total of 15 subjects (7 males and 8 females) with an average age of (23.27 ± 2.37) years were recruited for the experiment, and each subject completed three trials. During the presentation of the film clips, the subjects' EEG signals were recorded using a 62-channel EEG electrode cap based on the international 10-20 system. The electrode array amplifies the raw EEG signals and transmits them to the preprocessing module. The EEG signals were sampled at a frequency of 1000 Hz. The experimental procedure is illustrated in Figure 1. After viewing each film clip, the subjects completed a questionnaire to report their emotional responses. Only the samples that effectively evoked the target emotion, as indicated by the subjects' feedback, were considered valid for analysis.

(2) SEED-IV (Zheng et al., 2019): The dataset consisted of EEG and eye movement data from 15 participants, encompassing four emotions: happiness, sadness, neutrality, and fear. Each participant completed three separate sessions on different days, with each session comprising 24 movie clips. The EEG signals were sampled at a frequency of 1000 Hz. Figure 2 illustrates the experimental procedure.

(3) DEAP (Koelstra et al., 2011): In this study, 32 participants viewed 40 emotionally stimulating videos, each lasting 60 seconds. The experiment recorded EEG signals from 32 channels and peripheral physiological signals from eight channels. Following the video presentation, participants provided ratings for their emotional states. Valence values above five were manually labeled positive, while others were classified as negative. Figure 3 depicts a representative trial from the DEAP dataset.

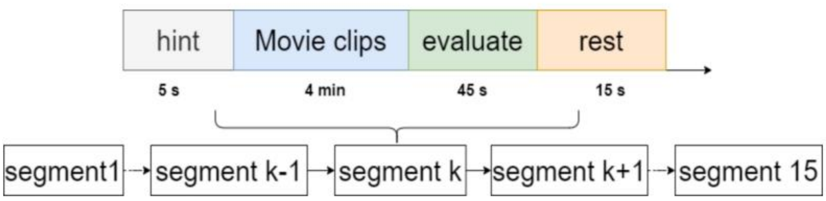

Figure 1 The experimental flow of SEED

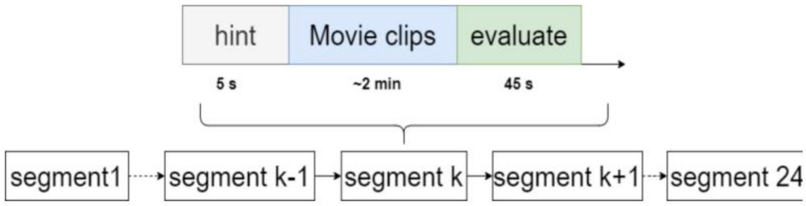

Figure 2 The experimental flow of SEED-IV

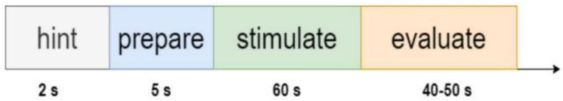

Figure 3 Time axis of a single trial in DEAP

2.2 Preprocessing

Only the data collected when the target emotion was elicited was utilized based on the participants' stress response. Initially, the original EEG data was downsampled to 200 Hz. Subsequently, blinking artifacts in the EEG data were manually eliminated using the recorded electrooculogram as a reference. To minimize the impact of noise and other interference on the EEG signals, a band-pass filter ranging from 0.3 Hz to 70 Hz was applied. Finally, the data was segmented into one sample per second to facilitate analysis and interpretation.

The study validates the efficacy of differential entropy (DE) in comparison to differential asymmetry, rational asymmetry, and energy spectrum (Duan et al., 2013). For a specific frequency range within a fixed-length EEG signal, the DE feature (Shi et al.,2013) is approximately equivalent to the logarithm of the power spectral density feature (Zheng & Lu, 2015). Additionally, under the assumption that the random variable follows a Gaussian distribution $N(\mu, \sigma^2)$, the feature can be expressed as follows:

$$h(x) = -\int_{-\infty}^{+\infty} \frac{1}{\sqrt{2\pi\sigma^2}} exp\frac{(x-\mu)^2}{2\sigma^2} log\frac{1}{\sqrt{2\pi\sigma^2}} exp\frac{(x-\mu)^2}{2\sigma^2} dx = \frac{1}{2} log2\pi e\sigma^2 \quad (1)$$

In the calculation of DE, e represents the Euler constant, and σ represents the standard deviation of the time signal. DE is equivalent to the logarithm of a specific frequency band energy spectrum when the time series follows a Gaussian distribution (Zheng et al., 2019). After preprocessing, a 512-point short-time Fourier transform is applied to compute the DE features of EEG signals in five frequency bands: delta (1-3 Hz), theta (4-7 Hz), alpha (8-13 Hz), beta (14-30 Hz), and gamma (31-50 Hz).

To ensure the stability of emotion analysis, it is necessary to reduce the rapid fluctuations in the feature sequence. Studies have demonstrated the effectiveness of employing a linear dynamical system for smoothing feature sequences (Duan, et al., 2013).

After the initial processing steps, the EEG signals from SEED and SEED-IV datasets, consisting of 62 channels, are further transformed to have a feature dimension of $62 \times 5 = 310$ per second. The feature is then expanded to a final dimension of 1×310 to obtain the sample feature. Similarly, for the DEAP dataset with 32 channels, the EEG feature dimension per second is $32(\text{channels}) \times 5(\text{bands}) = 160$, and after expansion, the dimension becomes 1×160 for the final sample feature.

2.3 Manifold sorting feature selection method

The proposed MSFS is used to solve the problem of cross-subject prediction in EEG-based emotion recognition. This framework selects the most suitable channel features which are used for prediction and classification through the manifold sorting feature selection method to study the emotion classification of specific brain regions in EEG emotion recognition. In the remainder of this section, we describe the corresponding components of this framework in detail.

A. Classification framework

Figure 4 depicts the multi-source classification framework of MSFS for addressing the cross-subject prediction problem in EEG-based emotion recognition. As shown in the figure, the framework starts by performing MSFS channel selection on the source domain 1, obtaining the last selected channel features and training the corresponding source domain classifier. The labeled target domain data is then processed with the selected channels and fed into the source domain classifier to obtain the voting weights of source domain 1. Next, the unlabeled target domain data is processed with the selected channels and injected into the source domain 1 classifier to obtain the predicted results for the target domain based on source domain 1. The same procedure is applied to the remaining source domains to obtain the predicted results for the unlabeled data in each source domain. Finally, a voting scheme is employed to aggregate the predictions from different source domains and obtain the final prediction results for the unlabeled data.

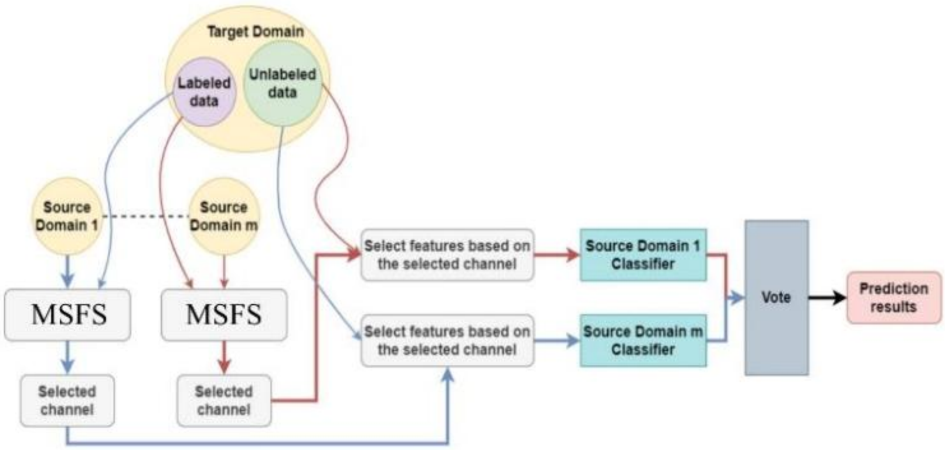

Figure 4 Classification framework based on manifold sorting feature selection

B. Manifold sorting

In the manifold sorting method, the source domain samples are represented as $\boldsymbol{\chi} = \{x_1, x_2, x_3, \ldots, x_n\} \in R^{m\times n}$, consisting of n samples in m dimensions, while the anchors which share the same space with the source domain samples, are denoted as $\boldsymbol{U} = \{u_1, u_2, u_3, \ldots, u_d\} \subset R^{m\times d}$. f represents the sorting function that maps x_i to the corresponding ranking scores f_i. Define $\boldsymbol{y} = [y_1, y_2, \ldots, y_n]^T$ as the initial vector and $y_i = 0$ in the context of feature selection. Euclidean distance between x_i and x_j denoted as $d(x_i, x_j)$, and $\omega_{ij} = \exp\{-d^2(\boldsymbol{x}_i, \boldsymbol{x}_j)/2\sigma^2\}$. ω_{ij} refers to the weight of the edge between samples i and j, $\boldsymbol{W} \in R^{n\times n}$ represents the adjacency matrix, and ω_{ij}denotes an element in the $\boldsymbol{W}$. $D_{ii} = \Sigma_{j=1}^{n}\omega_{ij}$, $\boldsymbol{D}$ is a diagonal matrix.

Therefore, the following objective function is derived.

$$\min_{f}\frac{1}{2}\left(\sum_{i,j=1}^{n}\omega_{ij}\left\|\frac{f_i}{\sqrt{D_{ii}}}-\frac{f_j}{\sqrt{D_{jj}}}\right\|^2+\mu\sum_{i=1}^{n}\|f_i-y_i\|^2\right) \tag{2}$$

where $\mu > 0$ is the regularization parameter. The optimal f can be obtained through a closed-form solution as shown below:

$$f = (\boldsymbol{I_n} - \alpha \boldsymbol{S})^{-1}\boldsymbol{y} \tag{3}$$

where $\alpha = \frac{1}{1+\mu}$, and $\boldsymbol{I_n}$ is an $n \times n$ identity matrix.

$$\boldsymbol{S} = \boldsymbol{D}^{-1/2}\boldsymbol{W}\boldsymbol{D}^{1/2} \tag{4}$$

where $\boldsymbol{D}$ is a diagonal matrix and each value is the sum of the values in the i-th row of $\boldsymbol{W}$.

The effective manifold sorting method improves the calculation of $\boldsymbol{W}$ by introducing a weight matrix $\boldsymbol{Z} \in R^{d\times n}$, which represents the underlying relationships between data points in $\boldsymbol{\chi}$ and anchor points in $\boldsymbol{U}$.

$$z_{ki} = \frac{\frac{K(|\boldsymbol{x}_i-\boldsymbol{u}_k|)}{\lambda}}{\Sigma_{l=1}^{d}K\left(\frac{|\boldsymbol{x}_i-\boldsymbol{u}_l|}{\lambda}\right)} \tag{5}$$

where K is the Epanechnikov quadratic kernel,

$$K_\lambda(t) = \begin{cases}\frac{3}{4}(1-t^2), & |t| \le 1\\ 0, & \text{Other}\end{cases} \tag{6}$$

$$\lambda(x_i) = \left|x_i - u_{[s]}\right| \tag{7}$$

$$\boldsymbol{W} = \boldsymbol{Z^T Z} \tag{8}$$

where $u_{[s]}$ refers to the anchor point that has the s-th closest Euclidean distance to the x_i.

When using the manifold sorting algorithm in MSFS, given an input sample x_{new} for querying, firstly, the Euclidean distances between x_{new} and each anchor point in $\boldsymbol{U}$ are computed and sorted, and then, z_{ki} is calculated based on Eqs. 5-7. The weight matrix $\boldsymbol{Z}$ has been calculated before for the sample features. We add the z_{ki} calculated for the new sample x_{new} to the weight matrix Z to get a new weight matrix $\boldsymbol{Z_{new}}$. The term $y_{n+1} = 1$ is added, and finally, the manifold sorting scores between the sample and the source domain samples are calculated according to Eqs. 3, 4 and 8.

The EEG signal is collected through an EEG cap equipped with 62 electrodes that comply with the international 10-20 system, as shown in Figure 5. In MSFS, we select T7, T8 as the query and use the corresponding manifold sorting scores as the basis for feature selection. According to reference (Zheng & Lu, 2015), T7 and T8 represent channels that can better reflect human emotions.

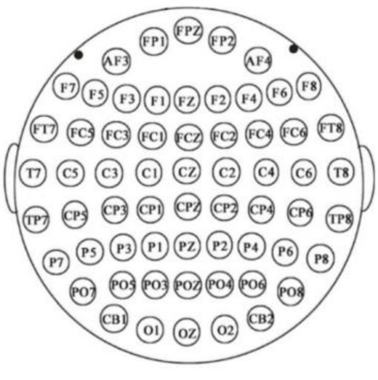

Figure 5 International 10/20 system

C. Workflow of MSFS

Figure 6 illustrates the workflow of MSFS in a specific source domain. Taking the electrode channel features selected for emotion category 1 as an example, the manifold sorting is performed on all samples in emotion category 1 using the T7, T8 channels as the reference. The top 8 electrode channels with the highest selection frequency are identified. Finally, the selected 8 electrode channels are analyzed for all samples in this category, and the electrode channel with the highest frequency of selection is chosen as the representative channel for emotion category 1 in this domain.

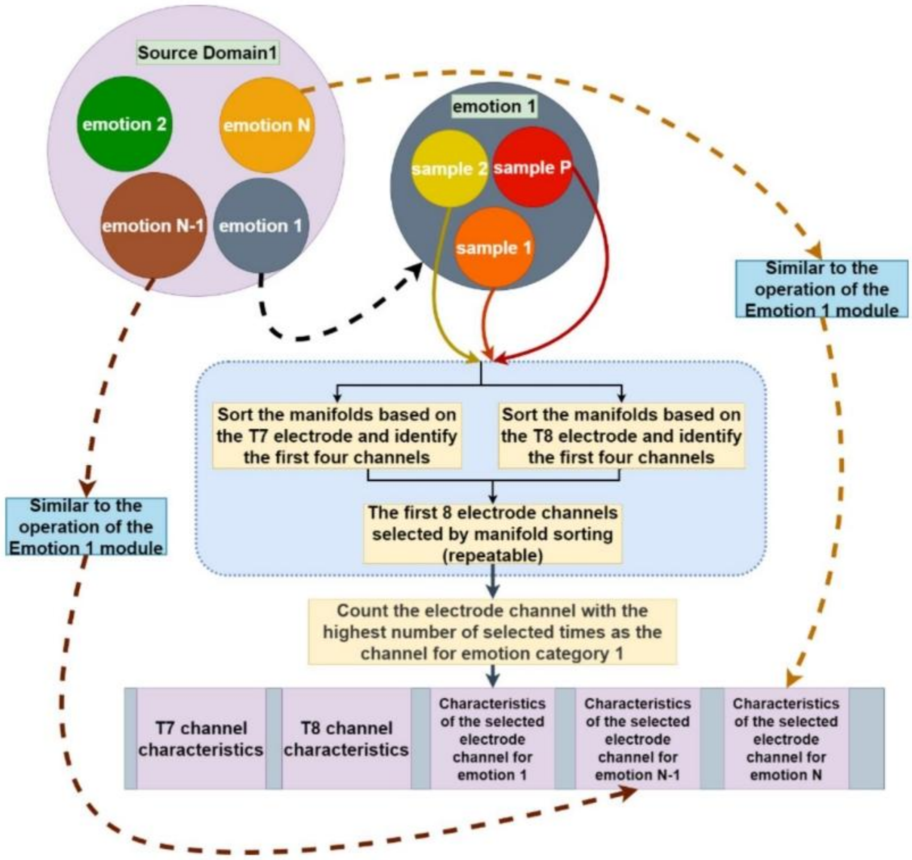

Figure 6 Flowchart of the proposed MSFS

The detailed steps of the MSFS process in the above procedure are described as follows. The source domain data S_i is divided into different classes C_1-C_N, the number of categories denoted as N, and i represents the *i*-th source domain. Given m source domains, there are $i \in [1, m]$. The *j*-th class samples in the *i*-th source domain are represented as $S_i^{C_j}$. Any sample from the *j*-th class is represented as $s_i^{C_j}(k), k \in [1, N_i^j]$, where N_i^j represents the number of samples in the *j*-th class of the *i*-th source domain. In Figure 6, P refers to the number of samples in the first class of the first source domain. Then, the individual channel features in $s_i^{C_j}(k)$ are treated as a single sample, and the entire set of channel features is considered as χ.

In the first step, $s_i^{C_j}(k)$ is transformed into a shape of the number of channels multiplied by the dimensionality of individual channel features based on the characteristics of each channel.

In the second step, the features of each channel are treated as $x_1, \ldots, x_{number\ of\ channel}$, and the corresponding weight matrix $\boldsymbol{Z}$ and f are calculated according to Eqs. 2-8, where N anchor points, represented as $u_1, \ldots, u_N$, are set and obtained through K-means clustering.

In the third step, the channel features of T7 and T8 are used individually as x_{new} for querying. The corresponding Euclidean distances between x_{new} and the anchor points in $\boldsymbol{U}$ are calculated and sorted. Then, based on Eqs. 5,6, z is computed and arranged after $\boldsymbol{Z}$ to form a new weight matrix $\boldsymbol{Z_{new}}$. $y_{n+1} = 1$ term is added, and the manifold sorting scores of T7 and T8 channel features with respect to the remaining channel features are calculated according to Eqs. 3,4,8.

In the fourth step, each channel's top four most relevant channels are selected individually. These selected channels are then combined to form a set of eight channels that have the most significant influence on this class (selected channels can be duplicated), preparing for the final voting to determine the channels with the greatest impact on this class. This step completes the manifold sorting feature selection for a single sample. The same process is applied to the remaining samples, and ultimately, the selected features for this domain as a source domain are obtained.

Next, MSFS processes the target domain based on the selected features from the corresponding source domain and performs classification. After making predictions for the target domain using each source domain, the final classification result for target domain samples is determined by a voting process.

Algorithm below shows the process of obtaining channel features selected for the *i*-th source domain through MSFS in the target domain.

Algorithm 1 Manifold sorting features selection

Input:

Data from the *i*-th source domain S_i

Initialization vector $\boldsymbol{y} = [y_1, y_2, \ldots, y_n]^T$

Final selected channel $F \in R^{(2+N)\times 1}$, $F(1) = \mathrm{T7}$, $F(2) = \mathrm{T8}$

for *i* = 1 to *m* **do**

  for *j* = 1 to *N* **do**

    $\boldsymbol{\chi} = C\left(s_i^{C_j}(k)\right)$

    $\boldsymbol{U} = K_{mean}(\boldsymbol{\chi})$

    According to Eqs. (2-8), input $\boldsymbol{U}$ and $\boldsymbol{\chi}$ to obtain $\boldsymbol{Z}$

    Calculate z based on Eqs. (5-7) for the characteristics of T7 and T8 channels

    $\boldsymbol{Z_{new}} = \begin{bmatrix} \boldsymbol{Z} \\ z \end{bmatrix}$, $\boldsymbol{y} = [y \quad 1]$

    According to Eqs. (3), (4) and (8) to obtain f

    Count the first 4 channels during T7 query and store them in $\boldsymbol{R}$

    Count the first 4 channels during T8 query and store them in $\boldsymbol{R}$

  end for

  $F(2+j) =$ The channel with the highest number of occurrences in $\boldsymbol{R}$

end for

Output:

Final selected channel F

2.4 Algorithms for comparison

This article observes the classification performance of using MSFS on some algorithms. In the paper, this article applies a leave-one-out strategy for cross-subject experimental evaluation: one subject is selected as the target domain sequentially, and the remaining subjects are attributed to the source domain. This article took the average accuracy of all subjects as the final classification result. The algorithms used include support vector machine (SVM), transfer component analysis (TCA) (Pan et al., 2010), balanced distribution adaptation (BDA) (Wang et al.,2017), correlation aligning (CORAL) (Sun et al., 2016) and joint distribution adaptation (JDA) (Long et al.,2013).

Parameter settings contributing to the highest mean classification accuracy are shown in Table 1. In addition, this article also compares MSFS with other feature selection methods, including F-value feature selection, feature selection based on credibility and consistency of hierarchical relationship (FSCCHI) feature selection, and minimum redundancy maximum relevance (MRMR) feature selection.

Table 1 Parameters setting of various methods

Methods	Parameters setting
support vector machine (SVM)	degree:3; gamma:0.3; cost:1; rbf
transfer component analysis (TCA)	lambda:5.2; d:20; primal;
balanced distribution adaptation (BDA)	lambda:0.2; d:20; primal;
joint distribution adaptation (JDA)	lambda:5.0; d:20; primal;
correlation aligning (CORAL)	—

3 Results

3.1 Classification performance

In the following, the effectiveness of MSFS in emotional EEG recognition cross-subject environments was verified through experiments. Figures 7, 8 and 9 respectively show the impact of MSFS and without MSFS on the average accuracy of all subjects under the five classification algorithms on three datasets. Figures 10 and 11 describe the impact of the MSFS algorithm and the other three feature selection algorithms on the average accuracy under SVM and TCA respectively. It can be observed that most methods exhibited improved classification performance when using MSFS for feature selection. However, BDA showed a decrease in classification accuracy after applying the MSFS algorithm. Since the MSFS feature selection significantly reduced the sample feature dimensions in the SEED-IV dataset from 310 to 6 dimensions, BDA could extract more information from the discarded features by MSFS, leading to better classification performance without using the MSFS method. Although the performance of MSFS in the BDA method was not ideal in the SEED-IV dataset, it demonstrated promising results in most other methods and significantly reduced the dimensionality of sample features. Figure 9 shows the performance of MSFS on the DEAP dataset, where it can be observed that MSFS did not perform satisfactorily on DEAP. After applying MSFS, the selected features exhibited poorer results than the original features in certain methods. This phenomenon can be attributed to the fact that the MSFS methods used T7 and T8 channels as the reference points for queries, which are known to be highly correlated with emotions in the SEED dataset rather than being the optimal channels in the DEAP dataset. Hence, the results in the DEAP dataset cannot effectively showcase the performance of the MSFS algorithm.

The following experiments are conducted to compare MSFS with other feature selection methods, aiming to demonstrate its good performance of MSFS and suitability for transfer learning algorithms. Figure 10 and Figure 11 present the experimental results in the SEED dataset. Figure 10 shows the classification performance of various feature selection methods in SVM, investigating the performance of MSFS in non-transfer learning methods. The figure shows that MSFS method outperforms the F-Value, FSCCHI method, and MRMR method. Figure 11 displays the classification performance of different feature selection methods in TCA, examining the effect of MSFS in transfer learning methods. Compared to other feature selection methods, MSFS consistently achieves superior results.

Further comparison between Figure 10 and Figure 11 reveal that not all feature selection methods, such as the FSCCHI and MRMR methods, are suitable for transfer learning. These methods amplify the negative transfer effects, leading to inferior results. MSFS, by selecting brainwave channel features, can mitigate the negative transfer effects to some extent and reduce the impact of irrelevant or redundant feature transfer mappings on recognition performance.

To comprehensively evaluate the performance of the MSFS algorithm, additional metrics are used for performance comparison in this section, and the results are presented in Table 2 and Table 3. The F1 score is a metric commonly used in statistics to assess classification models' accuracy, combining precision and recall. A higher F1 score indicates a stronger classification model. Additionally, the Kappa value is an important indicator for measuring classification accuracy. It can be used for consistency testing and also to assess classification accuracy. The lower the Kappa value, the more imbalanced the confusion matrix. Under these metrics, the MSFS feature selection method improves the ACC, F1-Score, and Kappa coefficients for most methods on the SEED and SEED-IV datasets, indicating that the MSFS feature selection method performs well. However, on the SEED-IV dataset, the performance of the BDA method decreases after applying MSFS. This phenomenon may be related to the dataset and the method used. Firstly, the SEED-IV dataset is a four-class dataset, where each feature contains more information compared with the three-class features. Therefore, using the MSFS channel selection method results in the loss of corresponding data, leading to decreased accuracy.

Table 2 Summary of classification metrics for various methods on the SEED dataset with and without MSFS

Algorithms	Without MSFS			With MSFS		
	ACC	F1-score	Kappa	ACC	F1-score	Kappa
SVM	0.7637	0.7601	0.6452	0.7763	0.7726	0.6637
CORAL	0.7464	0.7434	0.6194	0.7744	0.7710	0.6609
TCA	0.7734	0.7713	0.6597	0.7869	0.7825	0.6797
BDA	0.8264	0.8253	0.7393	0.8341	0.8326	0.7510
JDA	0.7737	0.7718	0.6601	0.7866	0.7823	0.6794

MSFS: manifold sorting feature selection; SVM: support vector machine; CORAL:correlation aligning; TCA: transfer component analysis; BDA: balanced distribution adaptation; JDA: joint distribution adaptation; ACC: Accuracy

Table 3 Summary of classification metrics for various methods on the SEED-IV dataset with and without MSFS

Algorithms	Without MSFS			With MSFS		
	ACC	F1-score	Kappa	ACC	F1-score	Kappa
SVM	0.5075	0.4943	0.3355	0.5365	0.5218	0.3756
CORAL	0.5301	0.5200	0.3682	0.5658	0.5487	0.4141
TCA	0.5028	0.4890	0.3317	0.5314	0.5178	0.3703
BDA	0.5629	0.5447	0.4128	0.5325	0.5109	0.3706
JDA	0.4883	0.4760	0.3133	0.5315	0.5180	0.3704

MSFS: manifold sorting feature selection; SVM: support vector machine; CORAL:correlation aligning; TCA: transfer component analysis; BDA: balanced distribution adaptation; JDA: joint distribution adaptation; ACC: Accuracy

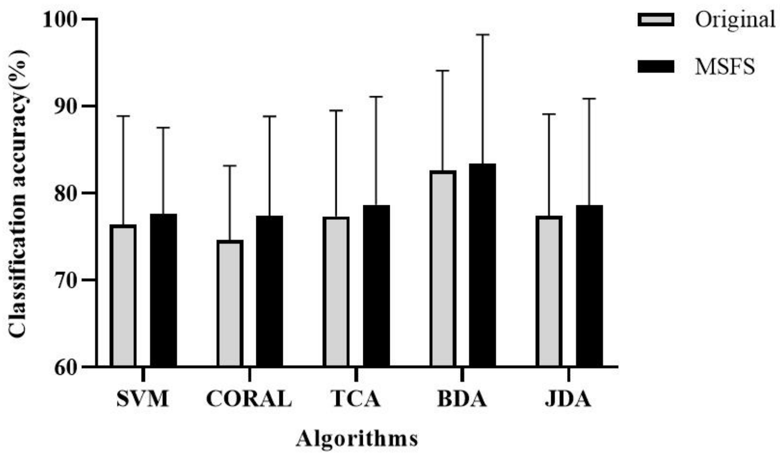

MSFS: manifold sorting feature selection; SVM: support vector machine; CORAL:correlation aligning; TCA: transfer component analysis; BDA: balanced distribution adaptation; JDA: joint distribution adaptation

Figure 7 Performance comparison of different methods before and after applying MSFS in the SEED dataset

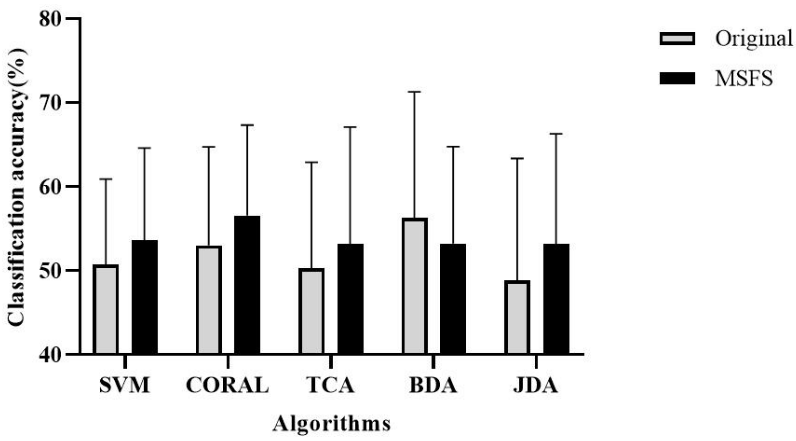

MSFS: manifold sorting feature selection; SVM: support vector machine; CORAL:correlation aligning; TCA: transfer component analysis; BDA: balanced distribution adaptation; JDA: joint distribution adaptation

Figure 8 Performance comparison of different methods before and after applying MSFS in the SEED-IV dataset

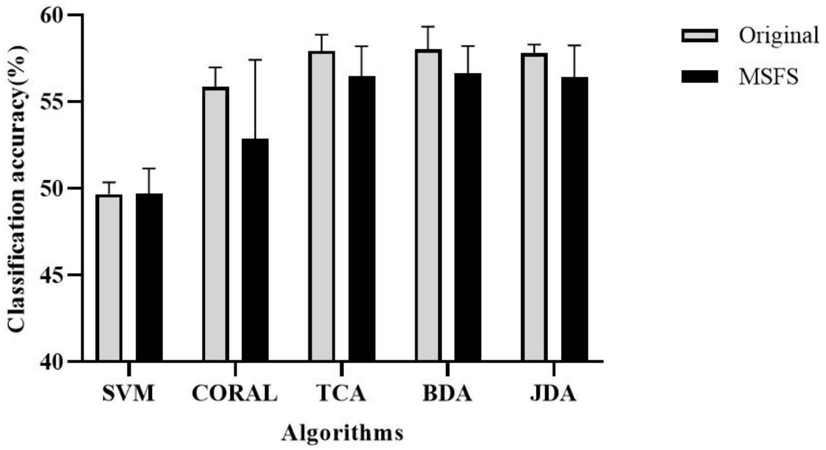

MSFS: manifold sorting feature selection; SVM: support vector machine; CORAL:correlation aligning; TCA: transfer component analysis; BDA: balanced distribution adaptation; JDA: joint distribution adaptation

Figure 9 Performance comparison of different methods before and after applying MSFS in the DEAP dataset

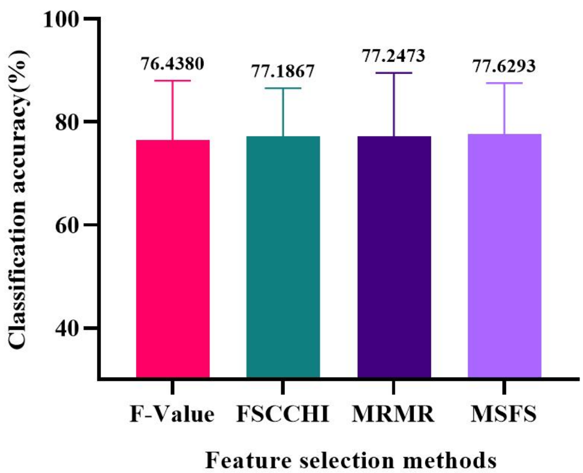

FSCCHI: feature selection based on credibility and consistency of hierarchical relationship; MRMR: minimum redundancy maximum relevance; MSFS: manifold sorting feature selection

Figure 10 Classification performance of various feature selection methods in support vector machine (SVM)

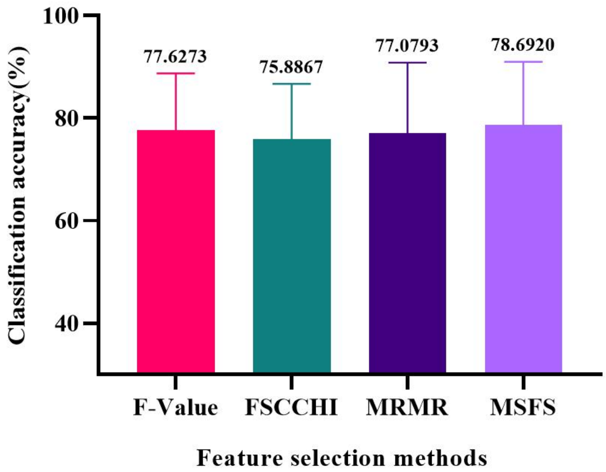

FSCCHI: Feature Selection based on Credibility and Consistency of HIerarchical Relationship; MRMR: minimum redundancy maximum relevance; MSFS: manifold sorting feature selection

Figure 11 Classification performance of various feature selection methods in transfer component analysis (TCA)

3.2 Parameter sensitivity

This section conducted experiments on the optimal number of channels corresponding to a category in the final set of features determined by MSFS. This experiment was conducted using the SEED dataset and the classification accuracy is the average accuracy of each of the 15 subjects as the target domain. The experimental results are shown in Figure 12, where 0 represents the result when only T7 and T8 channels were used as feature selection, 1 represents using only one channel for each category, 2 represents using two channels for each category, and so on. Figure 12 reveals that the best performance is achieved when the number of channels is set to 1. Additionally, the classification performance remains relatively stable as the number of channels corresponding to a category increases. Therefore, MSFS selects only one channel for each category. Furthermore, comparing the results of using only T7 and T8 channels as feature selection with the improved performance achieved by incorporating MSFS-selected channels demonstrates the effectiveness of MSFS from another perspective.

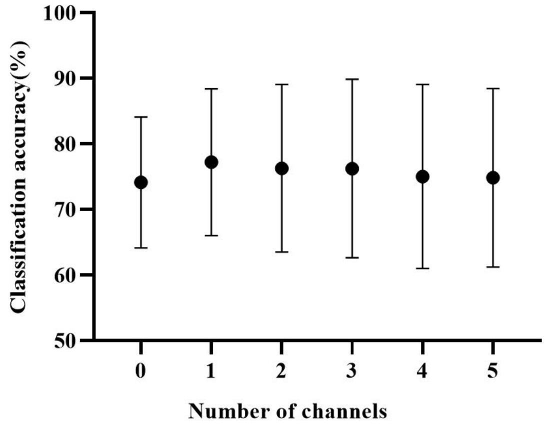

Figure 12 Performance of identifying the optimal number of channels corresponding to a category

3.3 Brainwave channels associated with different emotions

In this section, the MSFS algorithm was further evaluated by statistically analyzing the EEG channels selected for the emotions of happiness, neutrality, and sadness in the SEED dataset. The results, showing the most and second-most frequently selected channels for each emotion category, are presented in Figure 13. The purpose was to explore the channels most correlated with each emotion category. In Figure 13, the red channels T7 and T8 represent the reference channels for manifold sorting. The yellow channels FC2 and P8 are the most frequently selected feature channels for the negative emotion of sadness. The green channels TP7 and PO7 are the most frequently selected feature channels for neutral emotion. The blue channels FC4 and TP8 are the most frequently selected feature channels for the positive emotion of happiness. By comparing these results with the study by Zheng & Lu (2015), it can be observed that the brain regions selected by MSFS for emotion-related EEG channels largely coincide with their findings, providing additional evidence for the effectiveness of MSFS.

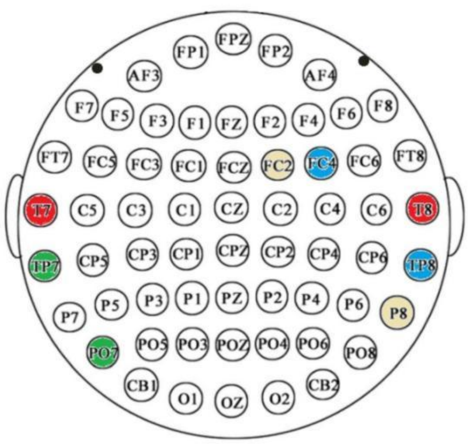

The red channels T7 and T8 represent the reference channels for manifold sorting; The yellow channels FC2 and P8 are the most frequently selected feature channels for the negative emotion of sadness; The green channels TP7 and PO7 are the most frequently selected feature channels for neutral emotion; The blue channels FC4 and TP8 are the most frequently selected feature channels for the positive emotion of happiness.

Figure 13 Schematic diagram of emotional channels

4 Discussion

In this paper, we develop a new feature selection framework named manifold sorting feature selection (MSFS), taking into account existing knowledge on the correlation between brain regions and emotion recognition. The paper addresses the problem of selecting domain-specific sentiment features by identifying channel features that are most correlated with other channels. At the same time, MSFS selects channels and trains respective classifiers for multiple source domains, and aggregates and predicts unlabeled target domains through voting to achieve multi-source classification problems, which is of great significance for the application of emotional brain-computer interfaces.

In general emotion recognition methods, they use the selection of time domain and frequency domain features, correlation analysis and feature selection in the feature space, and this paper based on the T7 and T8 channels found in the literature (Zheng & Lu, 2015) can better reflect human emotions. The MSFS method is proposed to select other channel features that are most relevant to the EEG emotional channel through manifold sorting. No matter what kind of classification algorithm is applied, the channel features selected according to MSFS are always the most relevant channel features for emotion recognition, which can always improve the accuracy of the classification algorithm. At the same time, the MSFS method can select the most relevant channels of positive, neutral and negative emotions, which can guide the brain-computer interface and help promote the application of brain-computer interface technology in emotional computing and human-computer interaction. Therefore, channel selection is also of paramount importance in effective BCI.

The paper studies various forms of emotional feature selection, and uses MSFS to conduct comparative experiments on five classification algorithms. The experimental results verify the effectiveness of MSFS in emotional EEG recognition in a cross-subject environment. Experimental results with MSFS showed that individual-specific emotions were associated with specific electrode channels. MSFS exploits the similarity of corresponding electrode channel distributions between new subjects and source domain subjects as a similarity comparison measure between source and target domains. It provides a novel approach to assess the similarity between domains in the context of EEG-based emotional scenes.

In addition, the MSFS method is compared with F-Value, FSCCHI and MRMR feature selection methods. The results show that MSFS achieves good results in the case of non-transfer learning algorithms and outperforms other methods in the context of transfer learning. This finding provides further evidence that the MSFS algorithm can enhance the transfer classification performance of EEG-based emotion recognition.

We found that in Table 3, when the SVM classification algorithm uses MSFS, the accuracy of the SEED-IV dataset is 23.98% lower than that of the SEED dataset, which may be due to the fact that the SEED dataset is a three-category sentiment classification dataset, while the SEED-IV dataset is a four-category data set. Emotion classification can express the classification performance as the ratio of accuracy to the classification probability of each category. SEED data set: 77.63%/33.33% = 2.33, SEED-IV data set: 53.65%/25% = 2.15. MSFS shows lower performance on the SEED-IV dataset, which may be because each of the four-category dataset SEED-IV features contains more information than the three-category features, while MSFS channel selection leads to more information loss in data. At the same time, SEED has a large amount of data, while SEED-IV has a small amount of data. The results show that the number of categories leads to the difference in accuracy.

Although our method achieves better performance than classification algorithms that do not use channel selection, the method has some limitations. Since there is no clear literature confirming the channels that reflect human emotions on the DEAP dataset, this paper does not verify the superiority of MSFS on the DEAP dataset. EEG signal processing and emotion classification models related to EEG emotion classification performance have attracted much attention. Our MSFS belongs to the category of EEG signal processing, and we used classification models of other algorithms for experiments, but did not propose a classification model suitable for MSFS. Huang et al. (2023a) and Li et al. (2021) proposed an automatic neural network architecture design method, while Huang et al. (2023b) propose to optimize the hyperparameters and block-based architectures in convolutional neural networks (CNNs) by genetic algorithms (GA). In future work, it is necessary for us to explore some automatic learning methods, such as neural structure search and hyperparameters optimization, and propose neural networks suitable for MSFS to improve the performance of emotion recognition.

5 Conclusion

This paper presents a MSFS method for emotion recognition, which utilizes existing knowledge about the brain and performs effective manifold sorting queries using brain-electrode channels most relevant to emotions as anchor points to obtain emotion-related EEG channel features. MSFS is a feature selection method that requires a small number of labeled samples from the target domain. It addresses the feature selection problem for new subjects in EEG-based emotion recognition by leveraging existing knowledge. A multi-source domain classification framework suitable for the MSFS feature selection method is proposed to further enhance its performance in multi-source domain scenarios. Our experimental results demonstrate that, on the SEED and SEED-IV datasets, the selected channel features by the proposed MSFS method are effective and lead to better classification performance than most other methods. However, several challenges remain for future work. Specifically, it is necessary to identify the most critical channels responsible for emotions in the human brain. While using the T7 and T8 channels as anchor points achieved good results in the SEED and SEED-IV scenarios, they are unsuitable for the DEAP dataset. Therefore, it can be inferred that although important for emotions, the T7 and T8 channels lack generalizability. Improving the selection of anchor channels in MSFS can address this issue. Furthermore, the method proposed by D.H., Li et al. (2022) to fuse various features and generate new composite features can also contribute to enhancing the overall performance of affective computing.

Conflict of interests statement

The authors declare that they have no conflict of interest regarding the publication of this article.

Acknowledgments

This work was partly supported by the Zhejiang Provincial Natural Science Foundation of China under Grant (No. LZ22F010003) and the National Natural Science Foundation of China under Grant (Nos. 62371172 and 62171171).

References

Ahmed, M. Z. I., Sinha, N., Ghaderpour, E., Phadikar, S., & Ghosh, R. (2023). A novel baseline removal paradigm for subject-independent features in emotion classification using EEG. *Bioengineering*, *10*(1), 54. https://doi.org/10.3390/bioengineering10010054

Chen, J., Li, H., Ma, L., Bo, H., Soong, F., & Shi, Y. (2021). Dual-threshold-based microstate analysis on characterizing temporal dynamics of affective process and emotion recognition from EEG signals. *Frontiers in Neuroscience*,*15*, 689791. https://doi.org/10.3389/fnins.2021.689791

Cheng, C., Zhang, Y., Liu, L., Liu, W., & Feng, L. (2022). Multi-domain encoding of spatiotemporal dynamics in EEG for emotion recognition. *IEEE Journal of Biomedical and Health Informatics*, *27*(3), 1342-1353. https://doi.org/10.1109/JBHI.2022.3232497

Dalgarno, B., & Lee, M. J. (2010). What are the learning affordances of 3-D virtual environments?. *British Journal of Educational Technology*, *41*(1), 10-32. https://doi.org/10.1111/j.1467-8535.2009.01038.x

Derdiyok, S., & Akbulut, F. P. (2023). Biosignal based emotion-oriented video summarization. *Multimedia Systems*, *29*(3), 1513-1526. https://doi.org/10.1007/s00530-023-01071-4

Duan, R. N., Zhu, J. Y., & Lu, B. L. (2013). Differential entropy feature for EEG-based emotion classification. 2013 6th International IEEE/EMBS Conference on Neural Engineering (NER). https://doi.org/10.1109/NER.2013.6695876

Huang, J. C., Zeng, G. Q., Geng, G. G., Weng, J., Lu, K. D., & Zhang, Y. (2023a). Differential evolution-based convolutional neural networks: An automatic architecture design method for intrusion detection in industrial control systems. *Computers & Security*, *132*, 103310. https://doi.org/10.1016/j.cose.2023.103310

Huang, J. C., Zeng, G. Q., Geng, G. G., Weng, J., & Lu, K. D. (2023b). SOPA - GA - CNN: Synchronous optimisation of parameters and architectures by genetic algorithms with convolutional neural network blocks for securing Industrial Internet - of - Things. *IET Cyber - Systems and Robotics*, *5*(1), e12085. https://doi.org/10.1049/csy2.12085

Huang, H., Xie, Q., Pan, J., He, Y., Wen, Z., Yu, R., & Li, Y. (2019). An EEG-based brain computer interface for emotion recognition and its application in patients with disorder of consciousness. *IEEE Transactions on Affective Computing*, *12*(4), 832-842. https://doi.org/10.1109/TAFFC.2019.2901456

Koelstra, S., Mühl, C., Soleymani, M., Lee, J.S.,Yazdani, A., Ebrahimi, T., Pun, T., Nijholt, A. & Patras, I. (2011). DEAP: A database for emotion analysis using physiological signals. *IEEE Transactions on Affective Computing*, *3*(1), 18-31. https://doi.org/10.1109/T-AFFC.2011.15

Li, C., Zhang, Z., Song, R., Cheng, J., Liu, Y., & Chen, X. (2021). EEG-based emotion recognition via neural architecture search. *IEEE Transactions on Affective Computing*, *14*(2), 957-968. https://doi.org/10.1109/TAFFC.2021.3130387

Li, D.H., Yang, Z.Y., Hou, F.H., Kang, Q.J., Liu, S., Song, Y., Gao, Q., & Dong, E.Z. (2022). EEG-based emotion recognition with haptic vibration by a feature fusion method. *IEEE Transactions on Instrumentation and Measurement*, *71*, 1-11. https://doi.org/10.1109/TIM.2022.3147882

Li, X., Zhang, Y.Z., Tiwari, P., Song, D.W., Hu, B., Yang, M.H., Zhao, Z.G., Kumar, N., & Marttinen, P. (2022). EEG based emotion recognition: A tutorial and review. *ACM Computing Surveys*, *55*(4), 1-57. https://doi.org/10.1145/3524499

Lin, W., & Li, C. (2023). Review of studies on emotion recognition and judgment based on physiological signals. *Applied Sciences*, *13*(4), 2573. https://doi.org/10.3390/app13042573

Long M, Wang J, Ding G, et al. (2013) Transfer feature learning with joint distribution adaptation. In Proceedings of the IEEE international conference on computer vision, 2200-2207.

Lv, Z., Zhang, J., & Epota Oma, E. (2022). A novel method of emotion recognition from multi-band EEG topology maps based on ERENet. *Applied Sciences*, *12*(20), 10273. https://doi.org/10.3390/app122010273

Makantasis, K., Liapis, A., & Yannakakis, G. N. (2023). The pixels and sounds of emotion: general-purpose representations of arousal in games. *IEEE Transactions on Affective Computing*, *14*(1), 680–693. https://doi.org/10.1109/TAFFC.2021.3060877

Moontaha, S., Schumann, F. E. F., & Arnrich, B. (2023). Online learning for wearable eeg-based emotion classification. *Sensors*, *23*(5), 2387. https://doi.org/10.3390/s23052387

Pan, S. J., Tsang, I. W., Kwok, J. T., & Yang, Q. (2010). Domain adaptation via transfer component analysis. *IEEE Transactions On Neural Networks*, *22*(2), 199-210. https://doi.org/10.1109/TNN.2010.2091281

Şengür, D., & Siuly, S. (2020). Efficient approach for EEG-based emotion recognition. *Electronics Letters*, *56*(25), 1361-1364. https://doi.org/10.1049/el.2020.2685

She, Q., Shi, X., Fang, F., Ma, Y., & Zhang, Y. (2023a). Cross-subject EEG emotion recognition using multi-source domain manifold feature selection. *Computers in Biology and Medicine*, *159*, 106860. https://doi.org/10.1016/j.compbiomed.2023.106860

She, Q., Zhang, C., Fang, F., Ma, Y., & Zhang, Y. (2023b). Multisource associate domain adaptation for cross-subject and cross-session EEG emotion recognition. *IEEE Transactions on Instrumentation and Measurement*, *72*, 1–12. https://doi.org/10.1109/TIM.2023.3277985

Shi, L. C., Jiao, Y. Y., & Lu, B. L. (2013). Differential entropy feature for EEG-based vigilance estimation. In 2013 35th Annual International Conference of the IEEE Engineering in Medicine and Biology Society (EMBC), 6627-6630. https://doi.org/10.1109/EMBC.2013.6611075

Shu, L., Xie, J.Y., Yang, M.Y., Li, Z.Y., Li, Z.Q., Liao, D., Xu, X.M., & Yang, X.Y. (2018). A review of emotion recognition using physiological signals. *Sensors*, *18*(7), 2074. https://doi.org/10.3390/s18072074

Song, T., Zheng, W., Song, P., & Cui, Z. (2020). EEG emotion recognition using dynamical graph convolutional neural networks. *IEEE Transactions on Affective Computing*, *11*(3), 532–541. https://doi.org/10.1109/TAFFC.2018.2817622

Sun, B., Feng, J., & Saenko, K. (2016). Return of frustratingly easy domain adaptation. In Proceedings of the AAAI Conference On Artificial Intelligence, *30*(1). https://doi.org/10.1609/aaai.v30i1.10306

Tao, W., Li, C., Song, R., Cheng, J., Liu, Y., Wan, F., & Chen, X. (2023). EEG-based emotion recognition via channel-wise attention and self attention. *IEEE Transactions on Affective Computing*, *14*(1), 382–393. https://doi.org/10.1109/TAFFC.2020.3025777

Wang, J., Chen, Y., Hao, S., Feng, W., & Shen, Z. (2017). Balanced distribution adaptation for transfer learning. 2017 IEEE International Conference On Data Mining (ICDM), 1129-1134. https://doi.org/10.1109/ICDM.2017.150

Xu, X., Jia, T., Li, Q., Wei, F., Ye, L., & Wu, X. (2023). EEG feature selection via global redundancy minimization for emotion recognition. *IEEE Transactions on Affective Computing*, *14*(1), 421–435. https://doi.org/10.1109/TAFFC.2021.3068496

Yin, Z., Liu, L., Chen, J., Zhao, B., & Wang, Y. (2020). Locally robust EEG feature selection for individual-independent emotion recognition. *Expert Systems with Applications*, *162*, 113768. https://doi.org/10.1016/j.eswa.2020.113768

Yin, Z., Zhao, M., Wang, Y., Yang, J., & Zhang, J. (2017). Recognition of emotions using multimodal physiological signals and an ensemble deep learning model. *Computer Methods and Programs in Biomedicine*, *140*, 93–110. https://doi.org/10.1016/j.cmpb.2016.12.005

Zhang, T., Wang, X., Xu, X., & Chen, C. L. P. (2022). GCB-net: Graph convolutional broad network and its application in emotion recognition. *IEEE Transactions on Affective Computing*, *13*(1), 379–388. https://doi.org/10.1109/TAFFC.2019.2937768

Zhang, T., Zheng, W., Cui, Z., Zong, Y., & Li, Y. (2019). Spatial–temporal recurrent neural network for emotion recognition. *IEEE Transactions on Cybernetics*, *49*(3), 839–847. https://doi.org/10.1109/TCYB.2017.2788081

Zheng, W.L., & Lu, B.L. (2015). Investigating critical frequency bands and channels for EEG-based emotion recognition with deep neural networks. *IEEE Transactions on Autonomous Mental Development*, *7*(3), 162–175. https://doi.org/10.1109/TAMD.2015.2431497

Zheng, W.L., Liu, W., Lu, Y., Lu, B.L., & Cichocki, A. (2019). EmotionMeter: A multimodal framework for recognizing human emotions. *IEEE Transactions on Cybernetics*, *49*(3), 1110–1122. https://doi.org/10.1109/TCYB.2018.2797176

Zhong, M. Y., Yang, Q. Y., Liu, Y., Zhen, B. Y., & Xie, B. B. (2023). EEG emotion recognition based on TQWT-features and hybrid convolutional recurrent neural network. *Biomedical Signal Processing and Control*, *79*, 104211. https://doi.org/10.1016/j.bspc.2022.104211